Ex vivo modeling of morphological, molecular and pharmacological tumor heterogeneity of metastatic colorectal cancer

Kushtrim Kryeziu[1], Solveig K. Klokkerud[1,2], Max Z. Totland[1], Seyed H. Moosavi[1], Henrik M. Reims[3], Christian H. Bergsland[1], Ina A. Eilertsen[1], Jørgen Smeby[1,4], Kristoffer Lassen[5,6], Kristoffer K. Lundesgaard[7], Trygve Syversveen[7], Morten Brændengen[8], Arild Nesbakken[1,2,9], Tormod K. Guren[4], Sheraz Yaqub[2,5], Anita Sveen[1,2], Ragnhild A. Lothe[1,2]

[1]Department of Molecular Oncology, Institute for Cancer Research, Oslo University Hospital, Oslo, Norway
[2]Institute of Clinical Medicine, Faculty of Medicine, University of Oslo, Oslo, Norway
[3]Department of Pathology, Oslo University Hospital, Oslo, Norway
4Department of Oncology, Oslo University Hospital, Oslo, Norway
[5]Department of Hepato-Pancreato-Biliary Surgery, Oslo University Hospital, Oslo, Norway
[6]Institute of Clinical Medicine, UiT The Arctic University of Norway, Tromsø, Norway
[7]Department of Radiology and Nuclear Medicine, Oslo University Hospital, Oslo, Norway
[8]Center for Cancer Medicine, Diakonhjemmet Hospital, Oslo, Norway
[9]Department of Gastrointestinal Surgery, Oslo University Hospital, Oslo, Norway

Supplementary figures

Supplementary Fig. 1

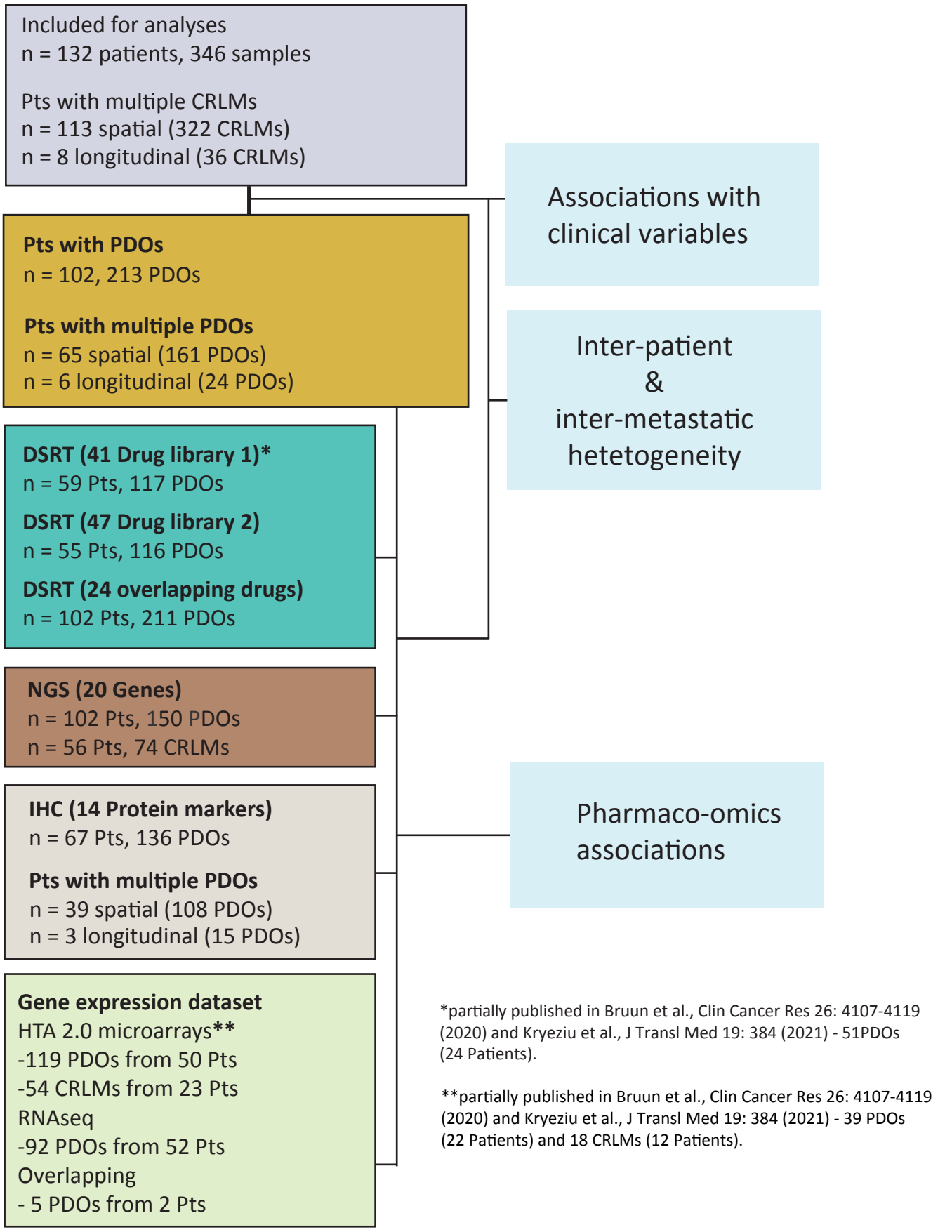

*partially published in Bruun et al., Clin Cancer Res 26: 4107-4119 (2020) and Kryeziu et al., J Transl Med 19: 384 (2021) - 51PDOs (24 Patients).

**partially published in Bruun et al., Clin Cancer Res 26: 4107-4119 (2020) and Kryeziu et al., J Transl Med 19: 384 (2021) - 39 PDOs (22 Patients) and 18 CRLMs (12 Patients).

Supplementary Figure. 1. Overview of the samples and methods used in the study. Pts - patients, PDO - patient-derived organoid, CRLM - colorectal liver metastasis, DSRT - drug sensitivity and resistance testing, HTA - Human Transcriptome Array, RNAseq - RNA sequencing, NGS - next-generation sequencing, IHC - immunohistochemistry.

Supplementary Fig. 2

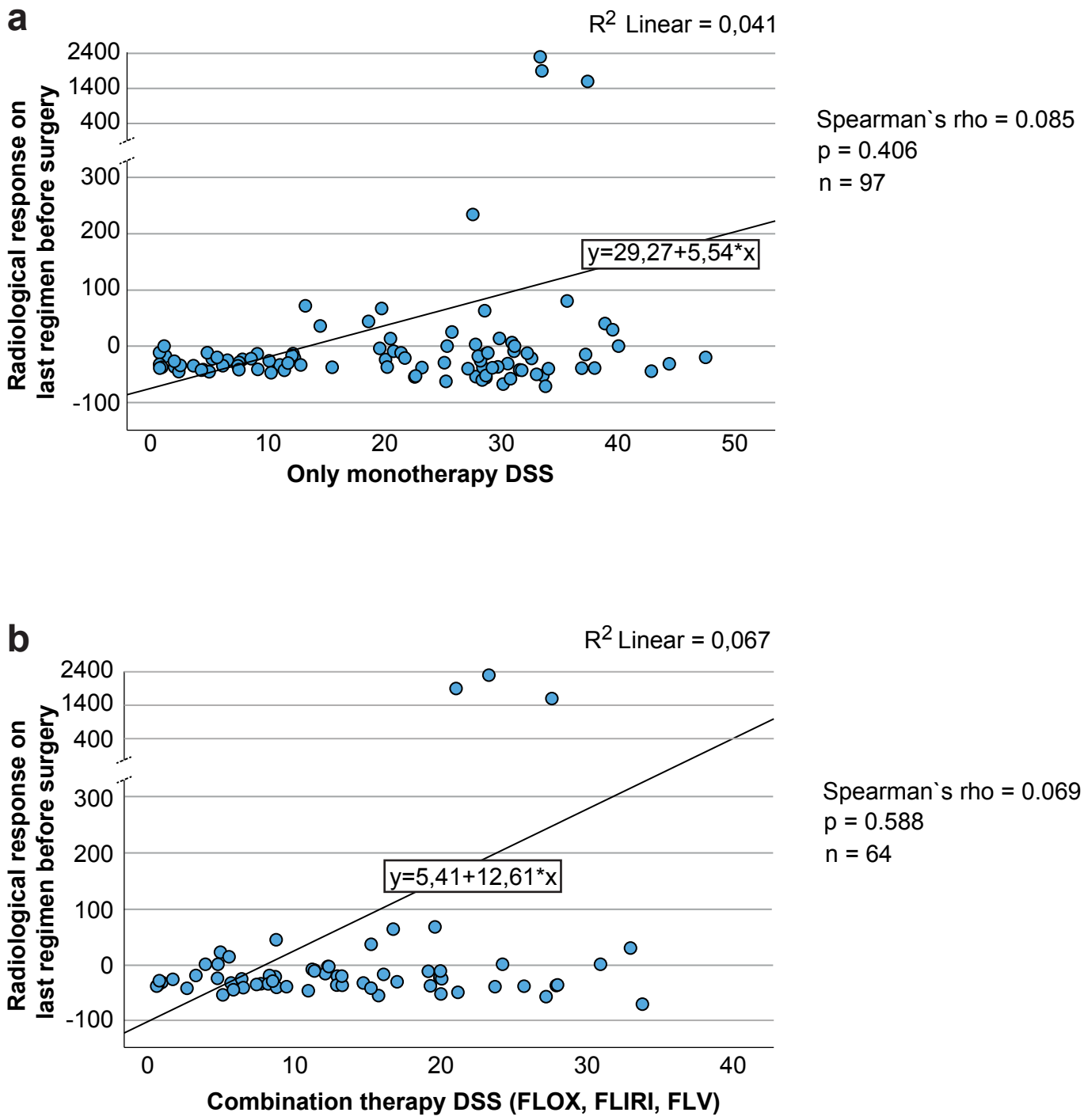

Supplementary Figure. 2. Radiological responses to neoadjuvant systemic therapy and ex vivo sensitivities to the correspond drug(s). a. Lesion-wise radiological response to neoadjuvant chemotherapy relative to *ex vivo* sensitivity for the corresponding agent(s) in the corresponding PDOs. The radiological measurements are given as % size change (in mm) relative to baseline, that is, 0 indicates no change, below 0 indicates reduction of tumor size (treatment response), and above 0 indicates increase of tumor size (progression on treatment). *Ex vivo* sensitivities were measured as drug sensitivity scores (DSS) for the corresponding single agents (**a**) or combinations (**b**). In (**a**), DSS for SN-38 was used for comparison in lesions treated with FLIRI/FOLFIRI +/- bevacizumab or anti-EGFR antibodies (n=56), DSS for oxaliplatin was used for FLOX/FOLFOX +/- bevacizumab or anti-EGFR antibodies, (n=39) and DSS for 5-FU was used for FLV (n=2). In (**b**), DSS for FLV was used for lesions treated with FLV, DSS for FLOX was used for FLOX/FOLFOX +/- bevacizumab or anti-EGFR antibodies, and DSS for FLIRI was used for FLIRI/FOLFIRI +/- bevacizumab or anti-EGFR antibodies.

Supplementary Fig. 3

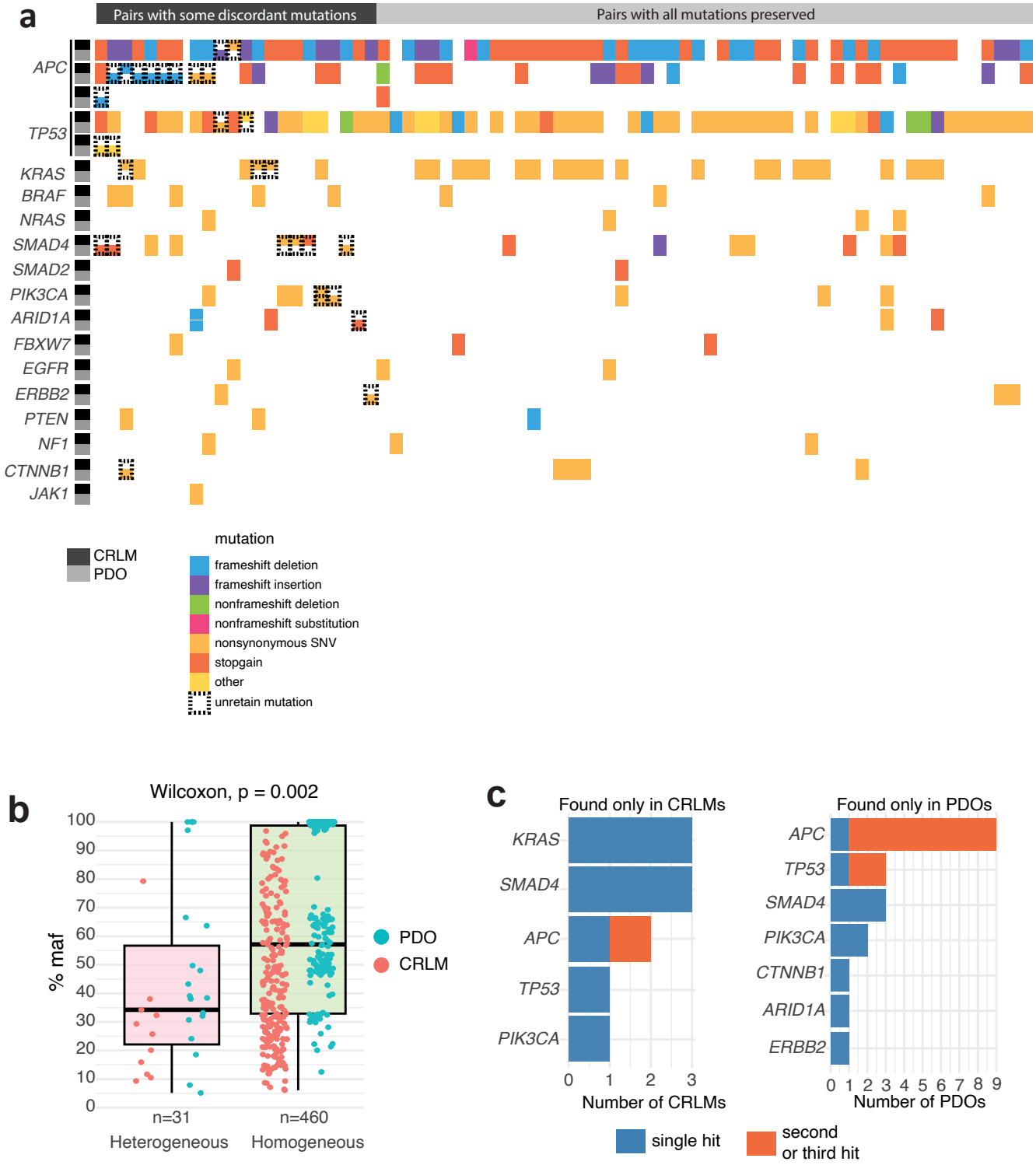

Supplementary Fig. 3. Comparison of somatic mutations between CRLMs and corresponding PDOs. a. Gene mutations compared between CRLMs and corresponding PDOs (n=74 sample pairs from 56 patients). Dashed outlines indicate discordant mutation status between the sample pairs. **b.** Box plot of mutant allele frequencies (maf) according to discordant (heterogeneous) and concordant (homogeneous) mutation status between paired PDOs and CRLMs. **c.** Bar plots of genes with discordant mutation status between paired CRLMs and PDOs.

Supplementary Fig. 4

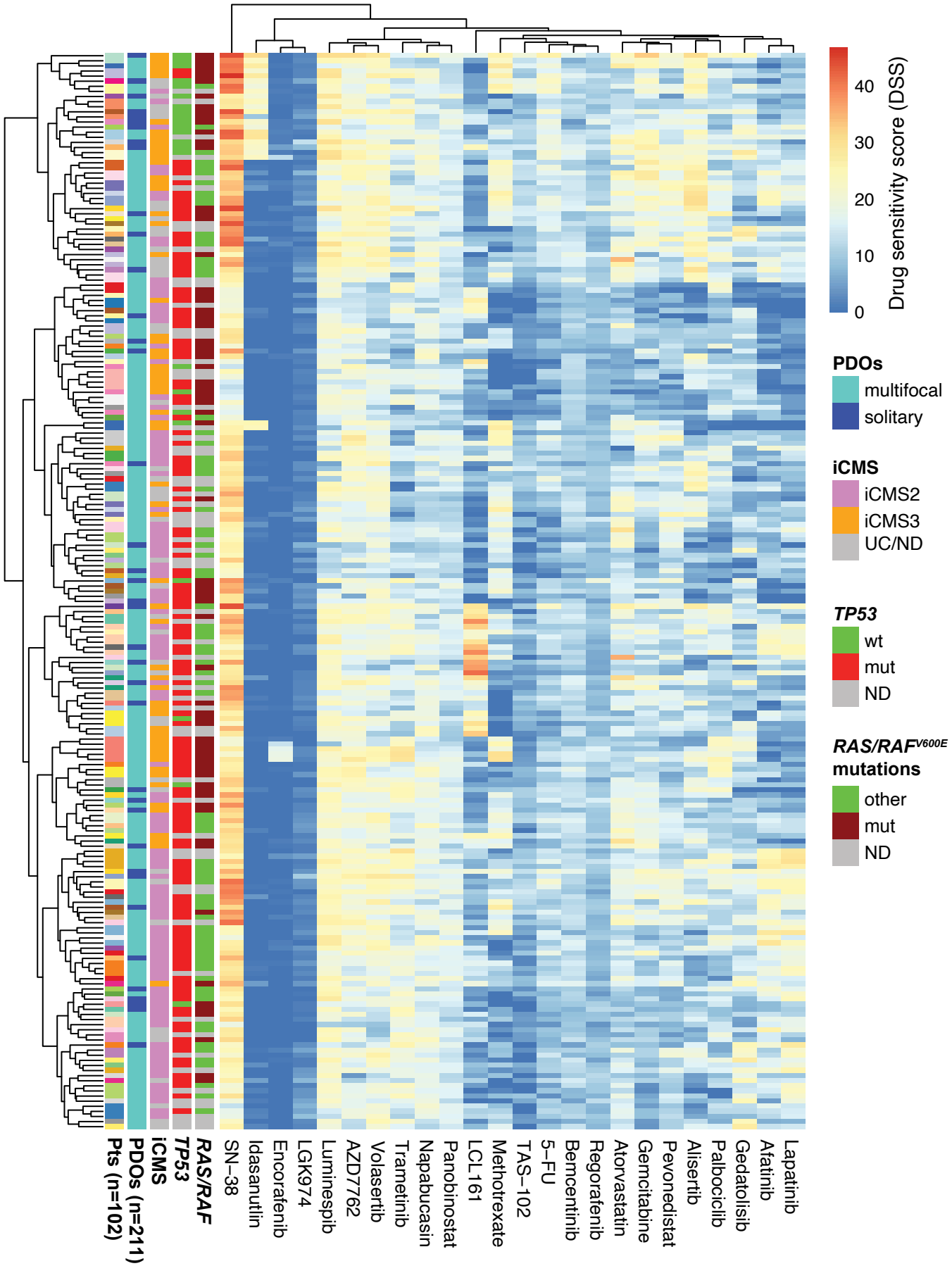

Supplementary Figure 4. Heat map and hierarchical cluster of drugs and PDOs. DSS values for 24 drugs in 211 PDOs from 102 Patients (Pts). Annotation bars indicate the mutation status of *RAS/BRAF*^{V600E} and *TP53*, as well as iCMS transcriptomic subtypes. Clustering was performed using the compete linkage method from the R package pheatmap v.1.0.12.

Supplementary Fig. 5

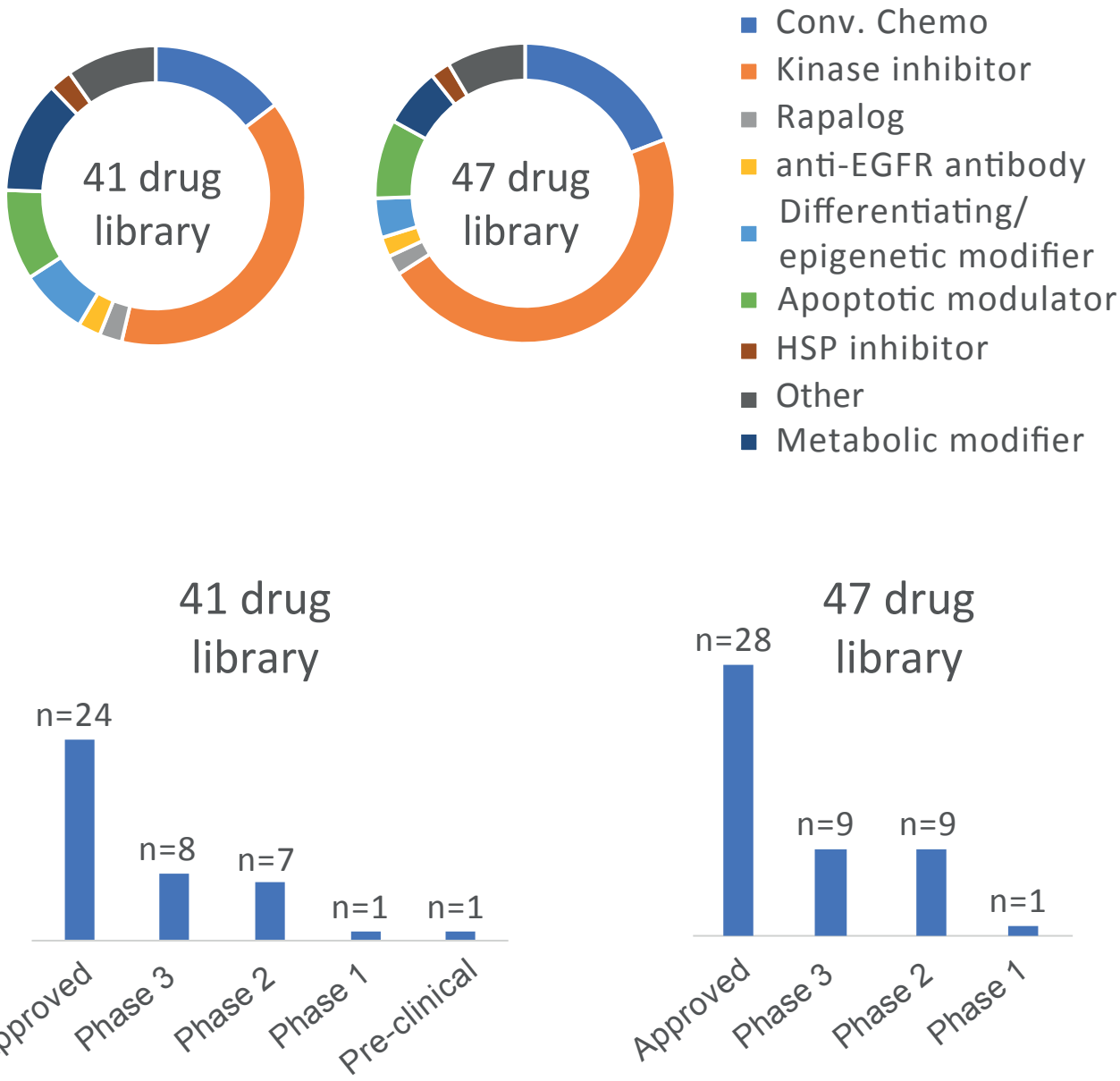

Supplementary Figure 5. Drug libraries. Mode of action and development status of drugs of library 1 (41 drugs) and library 2 (47 drugs) used in this study.

Supplementary Fig. 6

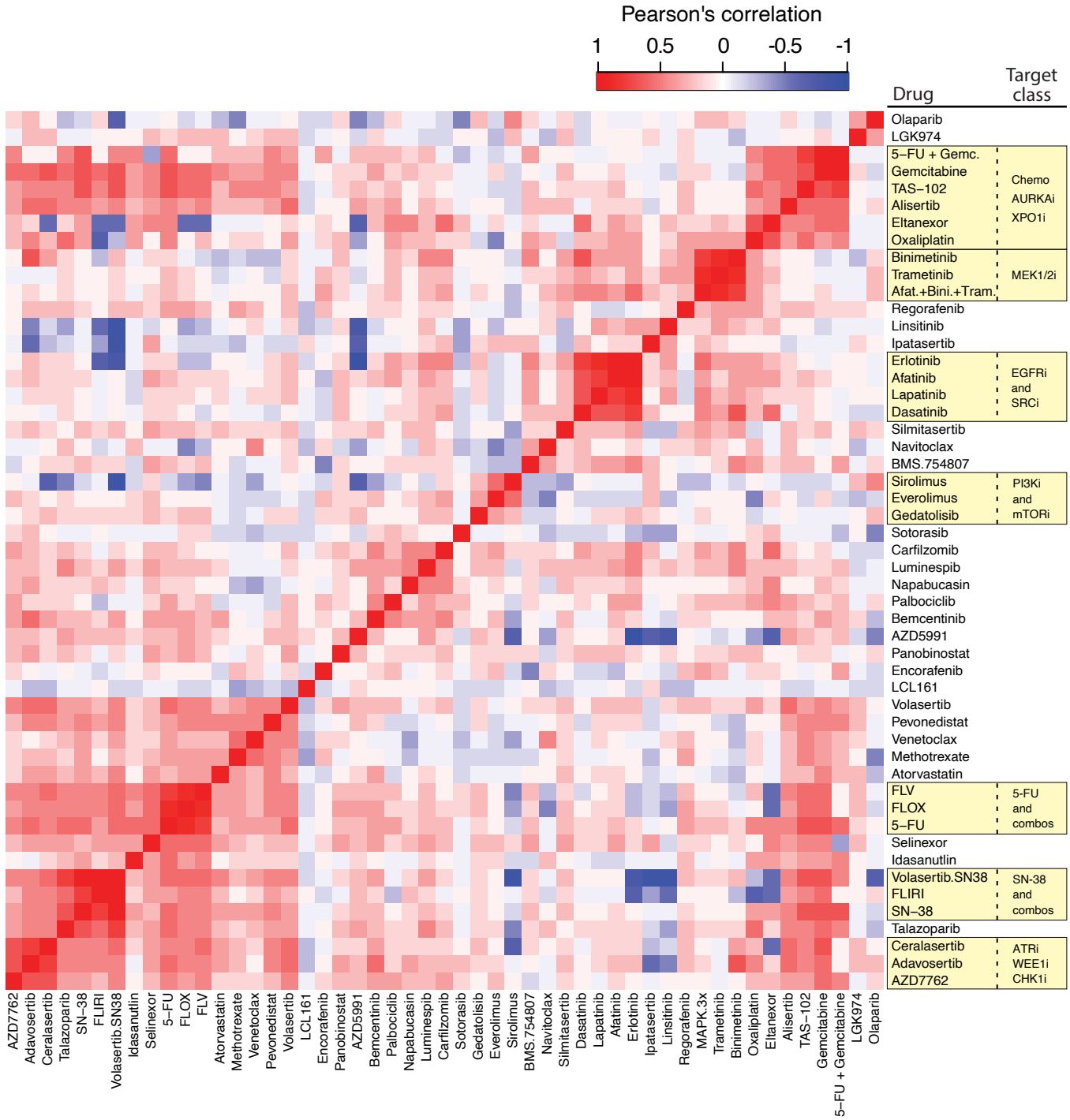

Supplementary Figure 6. Drug-drug correlation. Pearson correlation of 51 drugs and drug combinations from both libraries that passed the quality control criteria. Strongly correlating drugs or drug combinations are marked on the right based on their mode of action.

Supplementary Fig. 7

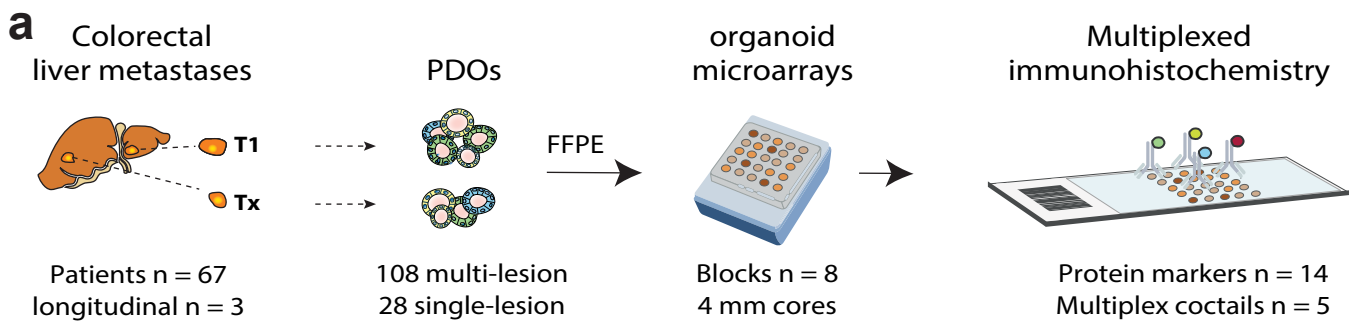

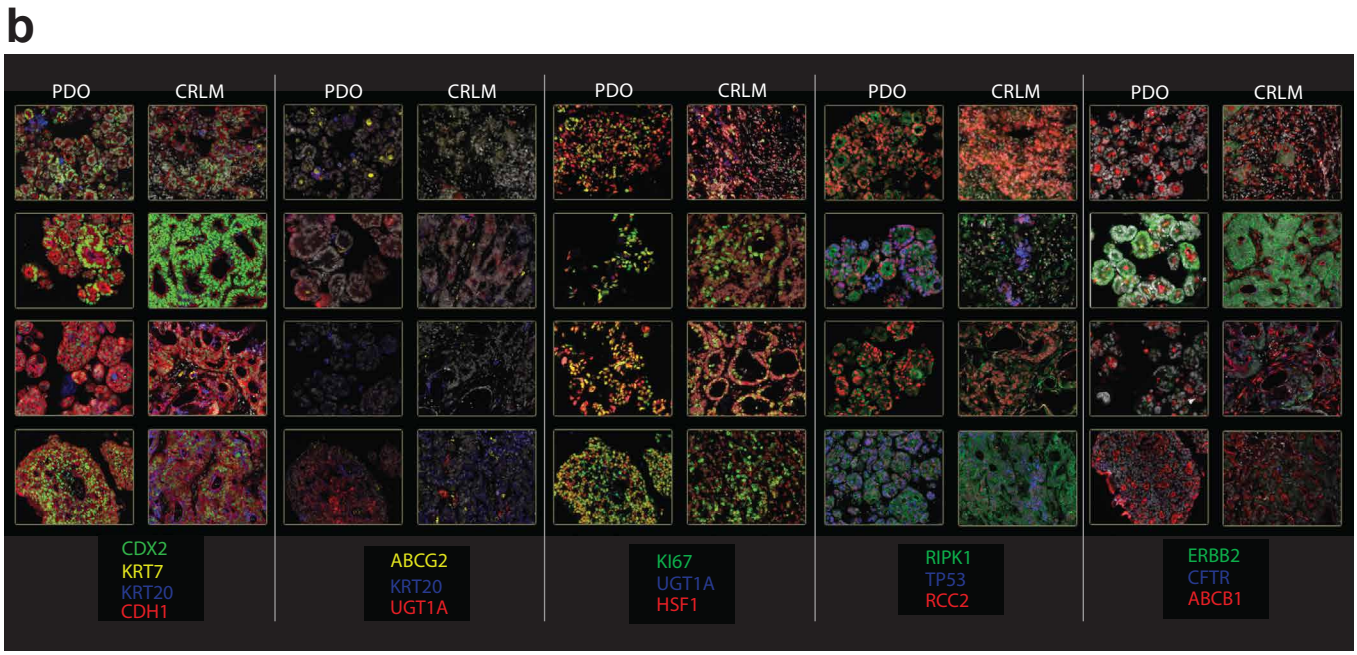

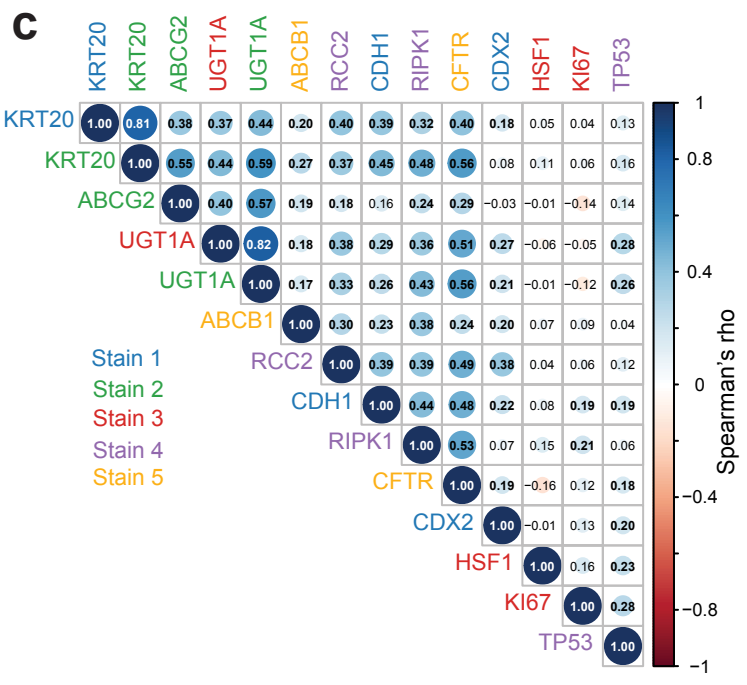

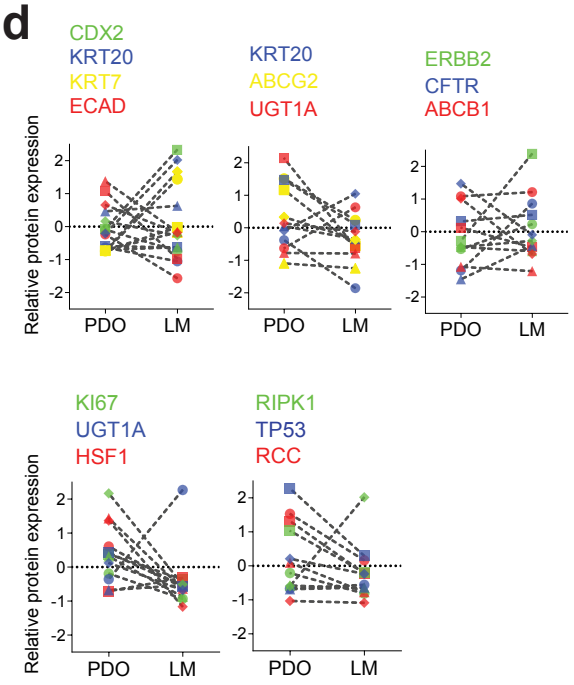

Supplementary Figure 7. Multiplex immunohistochemical characterization of protein expression in PDOs and matched CRLMs. a. Illustration of the process for creating the organoid microarray and performing multiplex immunohistochemistry. **b.** Five multiplex fluorescent immunohistochemistry cocktails analyzed in four PDOs and corresponding CRLMs from four patients. Nuclei were stained with DAPI and is shown in white, Scale bar 100 µm. **c.** Spearman correlation of the mean expression levels of 12 proteins in PDOs. Statistically significant correlation coefficients ($p<0.05$) are highlighted in bold. The correlations are ordered by hierarchical clustering. Proteins stained in the same multiplex are color-coded. **d.** Protein expression as centralized mean in matched PDOs and CRLMs indicated with distinct colors for the different multiplex cocktails.

Supplementary Fig. 8

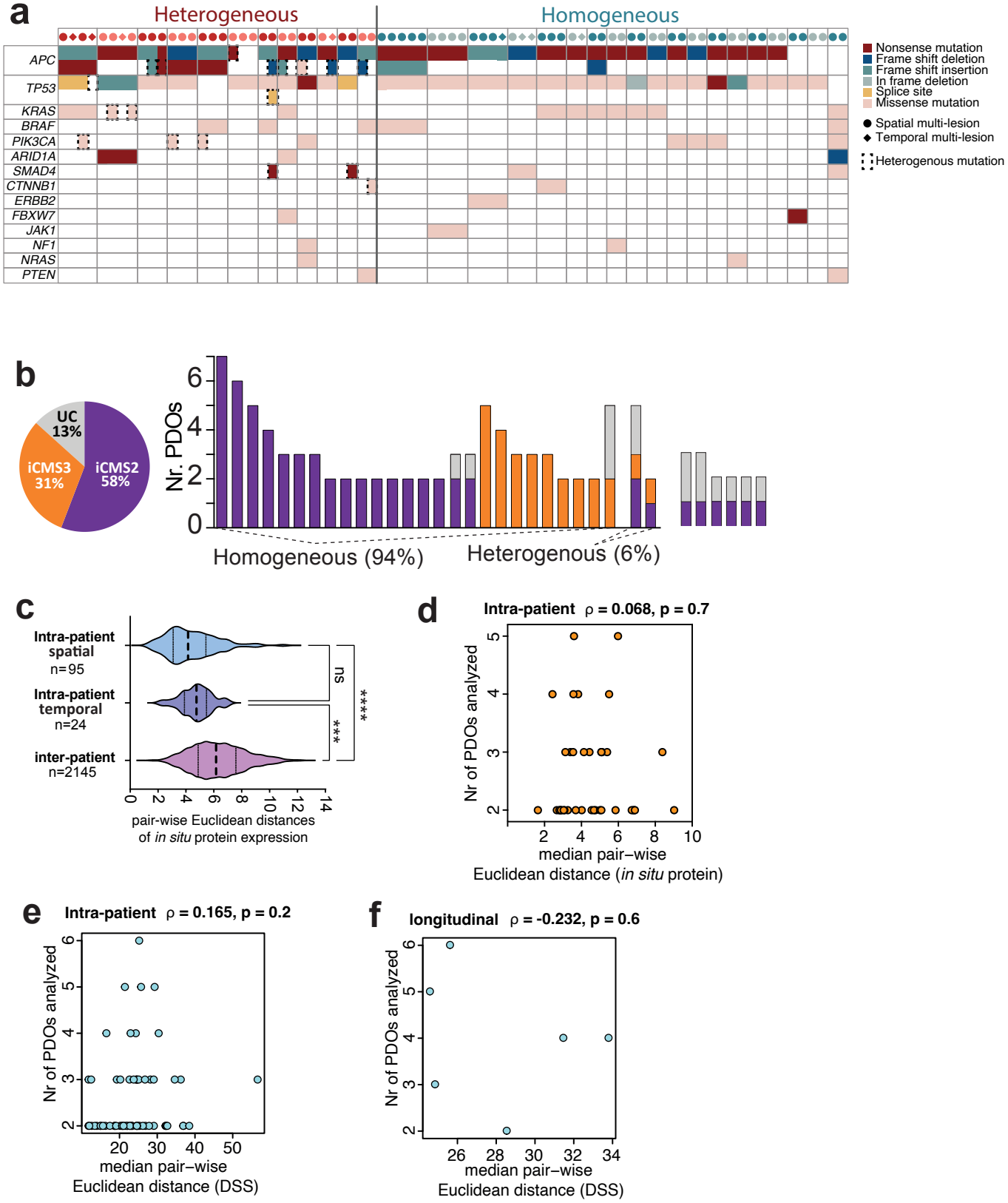

Supplementary Figure 8. Inter- and intra-patient heterogeneity in multi-lesion PDOs. a. Gene mutations in 32 PDOs from 12 patients with heterogenous mutations and 47 PDOs from 19 patients with homogeneous mutation profiles. PDOs from patients with multiple lesions are indicated with colored dots (spatial mutli-lesion) or diamonds (temporal multi-lesion) on top of the mutation map. Dashed line indicates the genes with a heterogeneous variant not found in all of the analyzed multi-lesion PDOs of the respective patients. **b.** Frequency and heterogeneity of iCMS classification between multi-lesion PDOs. **c.** Distribution of Intra-patient spatial, intra-patient temporal and inter-patient heterogeneity based on pair-wise Euclidean distances of 12 protein marker expressions based on multiplex IHC. The groups were compared with one-way ANOVA. Adjusted p values with Tukey's multiple comparison test, p<0.0001 (****). **d-f.** Spearman correlations between the number of lesions analyzed and median pair-wise Euclidean distances of DSS and in situ protein expression from multi-lesion PDOs.